Reevaluation of Historical Ocean Heat Content Variations With Time-Varying XBT and MBT Depth Bias Corrections

Masayoshi Ishii*

Frontier Research Center for Global Change
Japan Agency for Marine-Earth Science and Technology
Yokohama 236-0001, Japan

and

Masahide Kimoto

Center for Climate System Research
University of Tokyo
Kashiwa, 277-8586, Japan

For Journal of Oceanography

November 26, 2008 2nd Revision

Keywords: ocean temperature, XBT fall-rate equation, oceanographic observation, ocean heat content, objective analysis

Correspond to: M. Ishii,
3173-25 Showamachi, kanazawa-ku, Yokohama, 236-0001 Japan,
ism@jamstec.go.jp

* On leave from the Meteorological Research Institute of the Japan Meteorological Agency.

Abstract

As reported by former studies, temperature observations by expendable bathythermograph (XBT) and mechanical bathythermograph (MBT) appear to have positive biases as much as they affect major climate signals. These biases were not fully taken into account in the former ocean temperature analyses that have been used widely for the detecting global warming signals in the oceans. In this report, a methodology for eliminating the biases directly from the XBT and MBT observations is proposed. In the case of XBT observation, assuming that the positive temperature biases mainly originate from greater depths given by conventional XBT fall-rate equations than the truth, a depth bias equation is constructed by fitting depth differences between XBT data and more accurate oceanographic observations to a linear equation of elapsed time. Such depth bias equations are introduced separately for each year and for each probe type. An uncertainty of the gradient of the linear equation is evaluated by using a non-parametric test. The typical depth bias is $+10m$ at the $700m$ depth on average, which is probably caused by indeterminable various sources of the error in XBT observations as well as a lack of representativeness of fall-rate equations adopted so far. Depth biases in MBT are fitted to quadratic equations of depth by a similar manner to that of XBT. Correcting the historical XBT and MBT depth biases by these equations, a historical ocean temperature analysis is conducted. In comparison with the previous temperature analysis, large differences are found in the present analysis as follows; the duration of large ocean heat content in the 1970s shortens dramatically, and recent ocean cooling becomes insignificant. The result is also in better agreement with tide gauge observations.

1. Introduction

Historical ocean temperature analyses have been conducted using in-situ oceanographic observations by purely statistical methods (Levitus et al., 2000; Ishii et al., 2003; Willis et al., 2004; Smith and Murphy, 2007). The analyses are defined on a spatially uniform grid at a regular interval, and they are available for tens of years. In addition, the observational noise in the analyses is filtered out efficiently through processes of objective analysis adopted in each analysis. Therefore, the temperature analyses can easily be applied to studies for ocean climate changes. For example, global warming signals in the global oceans have been detected from these temperature analyses (Levitus et al., 2005; Ishii et al., 2006) and interannual variations of sea level (Lombard et al., 2005), and in verifying outputs of a model simulation for global warming signals (Sakamoto et al., 2005). The above-mentioned temperature analyses depend largely on the historical oceanographic observations, although the methodologies of the analysis are different from one another. A recent study by Gouretski and Koltermann (2007) suggests significant positive temperature biases in historical expendable bathythermograph (XBT) and mechanical bathythermograph (MBT) observations, which affects interdecadal variation of ocean heat content. These biases are not fully taken into account in the above temperature analyses.

Observation by XBT have been made widely over the global oceans since the late 1960s because of an easier measurement of temperature profile, compared with in-situ water sampling by hydrographic bottles. A cause of the biases pointed out by Gouretski and Koltermann (2007) is thought to be due to no simultaneous pressure measurements with the temperature observation. Instead of the pressure measurement, the depths for observed temperature are given by fall-rate equations, attributed to each XBT probe type. The equation gives depths (d) as a function of elapsed time (t) from the instant when the probe touches the water surface:

$$d(t) = bt - at^2, \tag{1}$$

where *a* and *b* are constants, given individually for XBT probe types. The equation (1) denotes that the probe falls linearly with time and simultaneously decelerated by decrease of probe weight due to wire loss. One possible cause of the temperature biases is positively biased depths given by the fall-rate equations.

In the mid 1990s, a fall-rate equation of popular XBT probe types, which is provided by several manufacturers, have been replaced by a new one based on results of field experiments (Hanawa et al., 1995). Observations by XBT were inspected for depth errors with accurate measurements by a conductivity, temperature, and depth (CTD) instrument simultaneously made with the XBT measurements in their experiments. This revision has a significant impact on the long-term trend and detection of the global warming signal. When the correction is not applied to all XBT data, eliminating already applied corrections from XBT data as well, annual global mean thermosteric sea level rise becomes smaller by 5–15 *mm* in most years after the mid 1960s (Ishii et al., 2006).

In the direct comparison between XBT and CTD measurements, the number of samples is generally of order 10 and those experiments were held in limited areas in the global oceans. Thus, such fall-rate equations may not work appropriately anywhere in the global oceans and anytime since the mid 1960s. Various source of the XBT errors should also be taken into account. For instance, Kizu and Hanawa (2002) reported errors from data recorders employed in the XBT observation.

In this study, an XBT "depth" bias correction is introduced in order to eliminate the positive "temperature" biases from long-term XBT observations (Gouretski and Koltermann, 2007), which remain even after applying the fall-rate equation by Hanawa et al. (1995). Similarly, a depth bias correction of MBT observation is also introduced. With these corrections, an ocean temperature analysis is conducted, following Ishii et al. (2006). In the subsequent sections, the detail of the XBT and MBT depth bias corrections newly introduced is described, and the depth biases detected by this approach will be presented. Conducting temperature analyses with the bias corrections, we demonstrate how the corrections affect ocean heat content on decadal and interannual time scales. Finally, a discussion is given of evidence supporting this approach.

2. Observational databases

Observed data and temperature and salinity climatology used in this study are the latest version of World Ocean Database (WOD05) and World Ocean Atlas (WOA05), respectively. The data sets are provided by the National Oceanographic Data Center of USA (NODC; Boyer et al., 2006). There are two types of data sets in WOD05: Observed level data and Standard level data, the former of which are used in this study. A near-real-time data archive archived through the Global Temperature-Salinity Profile Program (GTSPP) is also used, which compensates the data sparseness of WOD05 since 1990. The GTSPP data have been maintained by NODC under an international cooperation coordinated by the World Meteorological Organization and the Intergovernmental Oceanographic Commission. Furthermore, we added a set of XBT observations compiled by the Japan Oceanographic Data Center. These data are originally provided by the Japan Maritime Self-Defense Force (JMSDF) and are available from 1970 to 2003, which are not found in the above two data sets. Probe types T4 and T5 of Tsurumi Seiki have been used in the observations by JMSDF. The JMSDF data enable us to make statistics individually for probe type T4 of Tsurumi Seiki.

Comparing the latest WOD05 with the 2001 edition (WOD01), the number of profiles available at depths greater than 100 *m* increases particularly in the 1990s and recent years (Fig. 1). From the first appearance of XBT observation in 1966 until the mid 1990s, XBT has been a major instrument in the oceanographic observation. For a period before the XBT era, the MBT observation is dominant at the level of 100 *m* depth, and MBT observations had been made rather intensively in the 1970s and 1980s. In recent decades, Argo float data occupy more than a half of the observational data since 2003, while XBT observations have been made less frequently than before the mid 1990s.

Figure 1 near here, please.

3. XBT depth bias correction

a. A bias model

The XBTs are the most error prone oceanographic observations (Gouretski and Koltermann,

2007), because the depths of temperature are not measured directly by the XBT itself, as described above. In this study, we suppose that the XBT positive temperature biases are originated from depth biases and that the depth bias equation takes the same shape as Eq. (1):

$$\hat{d} = Bt + At^2. \tag{2}$$

Letter $\hat{d}$ represents biases in depth. One reason for the introduction of Eq. (2) is because the elapsed time is the primary measurement in the XBT observation. The coefficients of the quadratic equation, B and A, are estimated in a least-square sense from all available samples of depth differences between XBT and accurate observations such as CTD and hydrographic bottle together with corresponding elapsed time, t. The elapsed time used above can be computed from the inverse of the fall-rate equation (1) for a given depth of observation.

In the following, coefficients B and A are calculated for each XBT probe type and for each year. When conducting an objective analysis for historical temperature changes, depths of XBT observation are corrected by subtracting depth biases by Eq. (2).

Before the evaluation of the depth bias in XBT observation, the XBT fall-rate equation proposed by Hanawa et al. (1995) is applied to XBT data of probe types, T4, T6, T7, and DEEP BLUE if necessary, and to a part of XBT data whose probe types are unknown, following Conkright et al. (2001). Hence, depth biases given by Eq. (2) is an additional correction to that of Hanawa et al. (1995).

Probe types for a half of XBT observations are known, but unknown for a half of them, in the observational data sets used in this study (Table 1). Observations of unknown XBT probe types are also expected to be contaminated by positive temperature biases. In addition, our goal is not only to construct accurate XBT bias equations for each probe type, but also to eliminate temperature biases from XBT observations for an accurate historical temperature analysis. Hence, an additional type, *type unknown*, is introduced in the following. It is assumed that a single fall-rate equation is attributed

to XBT observations of *type unknown*. That is Hanawa et al.'s: Eq. (1) with $a = 2.25 \times 10^{-3}$ and $b = 6.691$.

Table 1 near here, please.

b. Box-averaged temperature profiles

Observed data are averaged monthly in box-shaped regions of the global oceans for individual XBT probe types and a mixture of CTD and hydrographic bottle (CTD+BOTTLE) for the period from 1966 to 2006. From the box averages, samples of depth difference between XBT and CTD+BOTTLE observations are taken for the estimation of the coefficients of Eq. (2). Before the box averaging, all observations are inspected and selected through quality control procedures adopted in our objective analysis scheme (Ishii et al., 2003, 2006).

The horizontal size of the box is set to be 1˚ longitude by 1˚ latitude over the globe. Depth differences more than 100 *m* were observed in actual XBT with CTD+BOTTLE observations at depths greater than 500 *m*. Therefore, the box is prepared up to 900 *m* depth for unbiased sampling of depth difference between XBT and CTD+BOTTLE box averages at 700 *m* depth. In addition, the thickness of the box is 10 *m* evenly from sea surface to 900 *m* for the sake of reduction of vertical interpolation error. According to our experience, errors from the vertical interpolation of observed and box-averaged values become substantially smaller in comparison with the resultant depth biases, in case of the thickness of 10 *m*.

In general, observations of XBT and CTD+BOTTLE used for the comparison locate far from each other maximumly by about 1.4-degree latitude distance, and there is a time lag within one month between them, as well. Meanwhile, it is presumable that oceanic temperature deviations from climatology have large spatio-temporal coherency exceeding 1˚-latitude distance and one month (Reynolds and Smith, 1994; Ishii et al., 2003). Therefore, when computing the box averages, we use observed deviations from the WOA05 climatology interpolated to the position and the date of the observation, rather than the use of full temperature values. By doing so, it is expected that errors in

the box average are minimized particularly in regions where the horizontal gradient of temperature is large and in months when the seasonal change is rapid.

There still remains large observational errors due mainly to ocean meso-scale eddies, instrumental errors, and human errors. Some of these are thought to be random error, and hence they can substantially reduce by using a number of samples when estimating the coefficients of the depth bias equation. The manufacturers state that an error in XBT temperature measurement is $\pm 0.2^{\circ}$C, and that the depth accuracy is the minimum of 5 meters or two percent of depth (Kizu et al., 2005). On the other hand, the accuracy of CTD and hydrographic bottle temperature observations is much higher than that of XBT, and it is within a range between $\pm 0.003^{\circ}$C and $\pm 0.02^{\circ}$C for temperature (Wyatt, Still, Barstow, and Gilbert, 1967; Fahrbach, 1989). Regarding the accuracy of depth of , it is better than ± 2 *m* for CTD and within ± 15 *m* for hydrographic bottle (Wyatt, Still, Barstow, and Gilbert, 1967; Fahrbach, 1989; Quadfasel et al., 1990). The error for hydrographic bottle denotes the maximum for the depth measurement range: 0 to $6,000$ *m* depth, and therefore smaller errors can be expected for depth measurements above $1,000$ *m* depth. In addition, the accuracy in the actual observation seems to be much better than the nominal accuracy, that is, the error reduces by a half, as Fahrbach (1989) reported. Moreover, these observations are made by trained members on ship and the sensors are regularly calibrated in general.

Within a calender month, observed deviations are averaged with weights which are the same as those used in a bilinear interpolation on the horizontal plane. Here, one observation is shared among the neighboring four boxes, and the weight is set to be the largest when the location of observation is the closest to the center of box. The sum of the weights for each observation is one. With this procedure, it is expected to minimize errors from distances between the center of box and the position of observation to some extent. It also functions as a spatial filter by which observational noise is somewhat reduced since observations in surrounding boxes are additionally used in the box averaging. Only box averages whose sum of weights exceeds 0.5 are used when taking a sample of depth

difference in a procedure described below.

c. Sampling of depth difference

The sampling of the depth difference between XBT and CTD+BOTTLE is conducted with the above-mentioned box averages as follows. Here, the climatology subtracted before the box averaging is added back to the box averages. For an XBT box-mean temperature at a level of the box in upper 700 *m* depth, a depth of the same temperature as that of the XBT is searched in a profile of CTD+BOTTLE box averages by interpolating linearly in the vertical. The difference of these two depth yields one sample for the estimation of the coefficients, together with elapsed time of the depth of the XBT observation. Such samples are taken from profiles of the XBT and CTD+BOTTLE box averages mutually in the same month and at the same location of the box. Similarly, an interpolated depth of XBT profile is computed for a CTD observation at a level of the box in upper 700 *m* depth. The above-mentioned procedure is expected to minimize errors in linearly interpolated depths on average particularly around thermocline where the curvature of temperature profile is large. The samples in the climatological mixed layer are not used, since the ocean temperatures fluctuate largely within a month there. It is also expected that XBT depth biases are small near sea surface since the biases are assumed to be a function of the elapsed time as Eq. (2).

d. Mean depth biases

Figure 2 shows profiles of XBT depth bias (thick solid) which are averages of the depth differences sampled by the above procedure over the whole period. The statistics is made for individual XBT types. Although there are a number of XBT probe types produced by several manufacturers: Sippican, Sparton, Tsurumi Seiki (TSK) and the others, the probe types appearing in the figure are the most dominant in WOD05 and GTSPP as listed in Table 1. It is found from the figure that the biases are larger at greater depths in general. It seems acceptable to fit them to an appropriate linear or quadratic equation. Interestingly, depths of XBT observation are not necessarily deviated positive, but they depend on the XBT types. There also appears dependence of depth bias on manufacturers;

depth biases of Sippican are large in general while those of Tsurumi Seiki are small. Mean depth biases averaged among all probe types are however positive and the positive depth biases appear to cause positive temperature biases that Gouretski and Koltermann (2007) reported. According to our estimation, the depth bias reaches about 10 *m* at 700 *m* depth on average.

The depth biases are 3–4 times smaller than root-mean-square differences (RMSDs; dotted), and the latter are due mainly to the observational and sampling noise. As inferred from this, the XBT depth bias estimation suffers from the noise. Therefore, a number of samples are required for the construction of the depth bias equation enough to overwhelm the noise. As discussed in the subsequent section, a lower limit of the number of samples is set to be $8,000$, and the all probe types listed in Table 1 satisfy this threshold.

Figure 2 near here, please.

e. A bootstrap test

Either the linear or the quadratic equations for $\hat{d}$ is adopted when conducting the objective analysis of historical temperature. In the linear case, the quadratic term, At^2, is ignored. To determine which equation is finally used, we introduced a non-parametric statistical test for errors in the coefficients estimated.

Because of the noisy box averages, we prefer to use coefficients, *B* and *A*, with small uncertainties rather than the coefficients realizing the best-fit regression to the noisy box averages. In addition, the error in depth difference used as sample is generally larger than that of depth of both XBT and CTD+BOTTLE observations. A bootstrap approach is taken in order to test the statistical significance in the estimation of the coefficients. From this test, we derive an appropriate number of of pairs of XBT and CTD+BOTTLE used for the determination of XBT depth bias equation. All available samples are collected within 10 years centered at each year at first. Selecting a set of samples randomly at a given number of samples, the coefficients of the equation are determined by a least squares fit. A thousand times of the trial are made for every $2,500$ sampling size from $2,500$ to $50,000$. Figure

3 shows 95% confidence levels for estimated coefficients B and A as a function of the number of samples in the case of *type unknown*. The plotted values are the mean among all the test over the whole period. Only for the case of the linear equation (thick solid), ranges between maximum and minimum 95% confidence levels during the whole period of the statistics are shown by shading. It is found from the figure that the uncertainty in the coefficient of the linear equation is much smaller than the case of the quadratic equation (thin solid and broken curves for coefficients, B and A, respectively). Values of 0.021 m/s and 0.00030 m/s^2 indicated by horizontal dotted line denote 95% confidence levels respectively for b and a of the Hanawa et al.'s fall-rate equation based on simultaneous XBT and CTD observations. These errors in b and a correspond to depth errors of 1.5 – 1.8 m at 500 m depth. The biases to be eliminated are on the order of 10 m as seen in Fig. 2. To achieve as small uncertainty as those of Hanawa et al. (1995), a required sampling size is around $5,000$ for the linear case on average, while it is about $30,000$ in the quadratic case. The difficulty in the estimation of the quadratic equation is due to the noise in the box-averaged data, that are probably affected by various sources of the errors. In addition, the ranges between max and min levels for the quadratic case are twice larger than those of the linear case (figure not shown). This implies that samples much more than $30,000$ are required to obtain coefficients with small uncertainty throughout the period. Data of *type unknown* could be a mixture of observations by various XBT probe types. Probably because of this, statistics for data of a single type such as T4, T7, and DEEP BLUE of Sippican result in smaller 95% confidence levels and narrower ranges of maximum and minimum levels than those for *type unknown* in general.

Figure 3 near here, please.

Therefore, the linear equation is adopted for the removal of the XBT depth bias. This enables us to make depth-bias correction equations for XBT probe types listed in Table 1. The threshold of the number of pairs is set to be $8,000$ at least and $15,000$ if possible. The threshold $15,000$ ensures that the 95% confidence interval is always less than 0.02. In the cases of XBT probe types other than *type unknown*, the threshold is good enough to ensure small estimation errors as well. A set of

8,000–15,000 samples are based on more than 85–165 observed profiles of XBT and CTD+BOTTLE individually. Thin solid curves in Fig. 2 show the residual of the differences between XBT and CTD+BOTTLE after applying the correction by the linear equation. As a result, the depth biases are reduced substantially.

f. Temporal changes in XBT depth biases

It is thought that there are various source of depth biases shown in Fig. 2. However, we do not know when and how such biases got mixed with XBT observation. Therefore, the coefficients of the linear depth bias equation are computed on a yearly basis for each XBT probe type. Samples in a given year are collected until the number of sample reaches 15,000 extending the range of the data search back and forth beyond the year under investigation. In order to avoid noisy temporal changes in coefficient *B*, samples for at least 5 years are used for determination of the coefficient. If the sampling size is smaller than the threshold, 8,000, even after the search for the whole period, the coefficients are not computed.

Coefficients of *B* for T4, T7, and DEEP BLUE of Sippican and *type unknown* are shown in Fig. 4, compared with depth corrections for shallow and deep XBT probe types calculated by Wijffels et al. (2008). The shallow (deep) XBT is the one whose maximum depth is less (greater) than or equal to 550 *m*. In their approach, depth bias corrections are given by multiplying a factor by depth of observation. The factor is defined respectively for shallow and deep XBTs as a function of year. To correct depth of observation is the same as the approach of this study. As seen commonly in all time series, maximum values of *B* appear in the latter half of the 1970s, the coefficients decrease in the latter half of the 1980s, and increase in recent years. The depth bias correction even for *type unknown* is necessarily conducted. When *B* is 0.3 m/s, an observed depth is corrected by about -24 *m* at 500 *m* depth. The differences among probe types including *type unknown* exceed the 95% confidence levels less than 0.02, in most years. The coefficient of T4 and *type unknown* is mostly invariant in time after 2000 because of poor sampling, and similarly in the case of T7 before 1970. Around these

periods, there exist large differences between the coefficients obtained by Wijffels et al. (2008) and this study.

Figure 4 near here, please.

Table 2 contains the coefficients of depth biases, B of the linear equation, for probe types whose number of samples exceeds $8,000$ (Table 1). In the case of probe type T6 of Tsurumi Seiki (TSK), the coefficient is always less than the estimation error, $0.02m/s$.

Table 2 near here, please.

4. MBT depth bias correction

In the case of MBT, the approach for the depth bias correction is the same as that of XBT except for a bias equation with a function of depth of observation not elapsed time as in the case of XBT. The depth biases ($\hat{d}$) of MBT reported by Gouretski and Koltermann (2007) are represented by a quadratic function of depth (z) as follows:

$$\hat{d} = Dz + Cz^2. \tag{3}$$

Coefficients C and D are calculated in a least-squares sense with samples of depth differences between box-averaged MBT and CTD+BOTTLE at depths above 250 m depth (Fig. 2 g) for the period from 1945 to 2006. No instrument types of MBT are considered here, and hence a single pair of the coefficients are computed as a function of year. Although linear bias equations are used for XBT, quadratic bias equations are adopted for the elimination of MBT depth biases. This is because the fitness to sampled depth biases is better than that of linear equation and because many samples are available for the estimation of the coefficients. Figure 5 shows a bootstrap test for MBT depth bias. Thick lines indicate mean values of the 95% confidence levels for D ($10^{-2}m/m$; solid) and C ($10^{-4}m/m^2$; broken), and upper and lower thin lines denote the maximum and minimum of the 95% confidence levels, respectively. Values indicated by these lines are interpretable as errors in meters at

100 *m* depth. Horizontal dotted line is drawn as a confidence level equivalent to the 95% confidence interval at 100 *m* depth of the Hanawa et al.'s fall-rate equation.

The error in bias estimated by Eq. (3) is a sum of errors originated from the both first and second term of Eq. (3). In the case of $80,000$, the maximum error is expected to be nearly equal to the error of Hanawa et al.'s fall-rate equation. The threshold number of samples is set to be $80,000$ in the case of the estimation of the MBT bias equation.

Figure 5 near here, please.

Table 3 displays the time series of coefficients C and D from 1950 to 1994. The values for C and D can be regarded as biases in meters at 100 *m* depth, evaluated respectively by the second and first terms of Eq. (3). The MBT depth bias at 100 *m* depth, as a sum of the linear and quadratic components, is about 2 *m* before 1980 and it gradually decreases closely to zero toward 1990. The MBT bias profile generally takes a parabolic shape. The linearity of bias profile appears relatively strong during the latter half of 1960s.

Table 3 near here, please.

5. Depth-bias corrected ocean heat content

Several ocean temperature analyses have been conducted for the period from 1945 to 2006, following the version number *6.2* of Ishii et al. (2006). In the objective analysis, the temperatures are defined on a $1^\circ \times 1^\circ$ grid at 16 levels from the sea surface to 700 *m* depth. The analyzed temperatures are deviations from the WOA05 climatology, optimally estimated by a three dimensional variational minimization technique (Ishii et al., 2003).

In the ver. *6.3*, a temperature analysis is conducted using the latest observational database (WOD05) and climatology (WOA05) in order to use more observations available after 1990 (Fig. 1). In ver. *6.2*, WOD01 and WOA01 were used. The long-term averages of a temperature analysis with the XBT depth bias correction (ver. *6.6*) differ significantly from the WOA05 climatological temperature as shown below. Hence, we introduced another temperature climatology which is computed from the average of temperature analysis of ver. *6.6* over the recent 40 years from 1961 to 2000.

An analysis with the new climatology is called version *6.7*, hereafter. In order to see the impact of the MBT depth bias correction, an additional analysis is introduced, in which only the XBT depth bias correction is adopted (ver. *6.6X*). The versions of the temperature analysis described above are summarized in Table 4.

Ocean heat content (OHC) discussed in this section is computed from the monthly temperature analysis above 700 *m* depth and WOA05 monthly salinity climatology. A grid-wise OHC at latitude ϕ is defined as a vertical integration of heating profile:

$$\int_{-700}^{0} \rho(T,S_c)C_p(T-T_{ref})R^2 cos(\phi)dz, \tag{4}$$

where $\rho(T,S_c)$ is the density of sea water for temperature T and climatological salinity S_c at depth z, C_p is a specific heat of sea water, T_{ref} is a reference temperature, and R is the radius of the earth. Although there are various choices of T_{ref} (*e.g.*, Levitus and Antonov, 1997 and Antonov et al., 2004), they are not so essential as to affect results presented in the following. In order to see explicit OHC changes caused by the depth bias equation, T_{ref} is set to be zero in this study.

Table 4 near here, please.

A temperature bias derived from the XBT depth bias is proportional to the vertical temperature gradient which varies from 0.02 to 0.2°C/*m* along climatological thermocline. The gradient is less than 0.05°C/*m* at depths below 300 *m* mostly, while large gradients exceeding 0.1 $^{\circ}$C/*m* appear around 100 *m* depth in the tropics along seasonal thermocline.

After introducing the XBT and MBT depth bias corrections in ver. *6.6*, cooling in the ocean temperatures are largely seen along thermocline depths in the subtropics (Fig. 6). This is reasonable because the depth biases become larger at greater depths and because the main thermocline locates around 200–400 *m* depths in the subtropics while it shallows in the tropics. This result motivates us to replace WOA05 used in the objective analysis of ocean temperature by another temperature climatology in order to minimize gaps between before and after the late 1960s when the XBT observation started. The MBT bias correction contributes to the OHC differences shown in the figure, but it is

small as discussed later. In the temperature analysis of Ishii et al. (2003, 2006), deviations from the climatology are analyzed. The new climatology, which is unbiased, is expected to yield an unbiased temperature analysis especially in a data-sparse period.

Figure 6 near here, please.

Figure 7 shows annual global mean time series of ocean heat content computed from the all versions of temperature analysis. The necessity of the replacement of the temperature climatology, mentioned with Fig. 6 above, is reconfirmed from the figure; large differences are seen since the late 1960s between the analyses of vers. *6.3* (dotted) and *6.6* (dash-dotted). The differences are mostly originated from the XBT depth biases, as the contribution of the MBT depth bias correction (solid line with circle) is relatively large before 1970 but small in later decades. By changing the climatology, an unbiased analysis is realized in the ver. *6.7* analysis (thick solid) before 1970.

Table 5 summarizes linear trends in OHCs and thermosteric sea levels derived from each version of analysis. The thermosteric sea level means sea level affected by thermal expansion and contraction of sea water, and it is computed with the temperature analysis in upper 700 *m* depth and climatological salinity (WOA05). The OHC trend of the ver. *6.7* analysis for 1955-2005 does not change significantly in comparison with ver. *6.2*. By contrast, the trend for recent 13 years (1993-2005) doubles almost. The reason is as follows. From the mid 1990s, the OHC differences between vers. *6.3* and *6.7* become small because the number of XBT observations gradually decreases (Fig. 1). This makes OHC larger in recent years than before the mid 1990s, and results in the trend twice larger than before. The replacement of the climatology in ver. *6.7* contributes to some extent but it is not a main factor over this period as seen in Fig. 7. When the MBT bias correction is not introduced (ver. *6.6X*), the long-term trend becomes smaller significantly in comparison with ver. *6.6*.

Table 5 near here, please.

A notable difference in OHC appears during the 1970s among the analyses. In the analyses prior to ver. *6.6*, OHC increases early in the 1970s and its anomaly is kept largely positive throughout the decades. In version *6.7*, OHC increases from 1970 similarly, but is slightly depressed in the latter

half of the 1970s, and increases again toward the maximum in 1980. This result does not contradict with Fig. 2 of Gouretski and Koltermann (2007). Probes T4 and T7 of Sippican were dominant over these three periods and they have large differences in depth from CTD+BOTTLE (Fig. 4).

In the previous analysis (ver. *6.2*), large ocean cooling appears since 2003 with a sizable amplitude (an OHC reduction indicated by thin line in Fig 7). This is partly due to a large cold bias of a small fraction of Argo floats having a large cold bias as Willis et al. (2008) reported. These Argo floats measure lower temperatures than expected particularly in the Atlantic Ocean. In ver. *6.3* and later, these Argo observations were withheld in the objective analysis. The difference between versions *6.2* and *6.3* since 2003 is mainly caused by the Argo data in question, while a differences between WOD01 and WOD05 used in the two analyses yields much less changes throughout the period as shown in Fig 7. Moreover, in ver. *6.6*, the recent ocean cooling becomes insignificant thanks to the introduction of the XBT depth bias correction. The reason of this is the same as that for the doubled OHC trend mentioned above. According to a study in which global mean sea level changes due to thermal expansion and contraction (thermosteric) are estimated from satellite sea surface height observations excluding ocean mass changes by satellite gravity measurements (Lombard et al., 2007), such cooling does not appear in time series of the satellite-derived thermosteric sea level.

Figure 7 near here, please.

6. Discussion

As seen in Figs. 6 and 7, the XBT depth bias correction affects the interannual to interdecadal variations of ocean heat content (OHC) as well as long-term averages of ocean temperature. However, it is hard to verify these changes directly by other oceanographic observations, whose spatio-temporal coverage is not enough for such an investigation in general. We have made a trial for such verification using sea level observations measured by tide gauges. Tide gauge observations used are the research quality data compiled by the University of Hawaii Sea Level Center.

Tide gauge observations suffer from various local effects, *e.g.*, ocean tide, coastal waves, crustal movement, especially at stations along continental coasts. In addition, dramatic changes by the

introduction of the depth bias correction were hardly seen in statistics between tide gauge data and thermosteric sea levels estimated from the temperature analysis at each tide gauge station, compare with Table 1 and Fig. 5 of Ishii et al. (2006). Hence, sea levels averaged over all available tide gauge stations located in islands were compared with thermosteric sea levels at dates and positions corresponding to the tide gauge observations. The thermosteric data are computed from the monthly temperature analysis and the WOA05 monthly salinity climatology. A target area for the verification is the tropical and subtropical Pacific between 30˚S and 30˚N, where the cooling due to the depth bias correction appear to be large (Fig. 6) and where the thermosteric effect is larger than the contribution of salinity to sea level change (Fig. 9 of Ishii et al., 2006).

Figure 8 depicts the time series of monthly sea level anomalies for tide gauge observation (dotted) and the corresponding thermosteric sea level anomalies (thin and thick solid lines respectively for vers. *6.3* and *6.7*). Tide gauge stations are adopted for the comparison if the data are available in more than 120 months for the period from 1950 to 2005. The tide gauge stations used for the comparison are shown by circle in Fig. 6. The three time series agree well with one another. In addition, the agreement between tide gauge and the ver. *6.7* analysis is better than that for version *6.3*, in particular, around 1975 and in years after 1985. The root-mean-square differences and correlation coefficients against the tide gauge observation are 16 *mm* and 0.77 for ver. *6.7*, respectively, while they are 19 *mm* and 0.68 for ver. *6.3*.

Following the discussion made by AchutaRao et al. (2007), we produce two evidences in support for the disappearance of positively deviated OHC during the 1970s seen in the previous temperature analysis (Ver. 6.2). One evidence is that dynamical models arranged for reproduction of the 20th century climate with global warming gases and volcanic forcing could not reproduce anomalous OHCs over this period (Fig. 1 of their manuscript). The other is an abnormally rapid increase of OHC at the beginning of the 1970s, seen in the *6.2* and *6.3* analyses (Fig. 7). AchutaRao et al. (2007) concluded that recent ocean cooling since 2003 is artificial because state-of-art dynamical models are unable to replicate changes of OHC from 2003 to 2005 (Fig. 3 of theirs), based on statistics of

2-year OHC changes. A similar conclusion is drawn after their discussion, because the OHC change at the beginning of the 1970s ($+4.5 \times 10^{22}$ *J* per 2 years) is the same size as that for the recent ocean cooling (-4.5×10^{22} *J* per 2 years).

Following the result of the bootstrap test (Fig. 3), linear equations were chosen for the depth bias correction. We made an additional analysis with quadratic equations with the same threshold number of XBT-(CTD+BOTTLE) pairs as that for the linear equations. In this case, the estimation errors are twice as large as the linear case (Fig. 3). Although the selection of the order of the depth bias equation affects the grid-wise OHCs; the differences between the two analyses are mostly within 30%, the global and basin-scale averages of OHCs were almost the same as each other. Therefore, at present, it is better to choose the linear equation for the removal of the depth bias since the biases defined by the quadratic equations involve large uncertainties.

There is no method for detection of depth biases in past XBT observations other than the approach taken in this study or ones similar to this approach (*e.g.*, Wijffels et al., 2008). Although the estimation of bias equation by our approach suffers from noise in box averages of XBT and CTD+BOTTLE observations, the bootstrap test ensures that a reliable bias equation can be obtained by increasing the number of samples used for the estimation. Needless to say, there is a great advantage in Hanawa et al. (1995) in which they used simultaneous XBT and CTD observations.

Figure 8 near here, please.

7. Conclusion

Depth bias corrections for XBT and MBT are introduced to the historical temperature analysis of Ishii et al. (2006) in order to remove positive temperature biases in XBT and MBT observations identified by Gouretski and Koltermann (2007). The results of this study suggests the necessity of reevaluation of interannual to decadal variations of ocean heat content as well as global warming trend particularly in recent decades.

Time-varying depth bias equations are constructed for each XBT probe type and MBT so as to reduce the differences between bathythermographs and CTD+BOTTLE observations, although our

knowledge is insufficient to specify the cause of the positive temperature biases. The correction depending on probe type is very necessary for a reasonable temperature analysis in regions of the ocean basins, since depth biases appear to be largely attributed to the probe types. Moreover, specific XBT probe types tend to be used in limited regions of the oceans. Also it is noteworthy that the depth bias equations obtained depend on the observational databases in this study. Accurate metadata on XBT probes are necessary for better understanding and estimation of XBT biases.

Observations by XBT as well as MBT are certainly important for long-term climate studies because of their spatio-temporal coverage. Efforts should continuously be made for a better use of them.

Acknowledgments.

The authors wish to thank Prof. K. Hanawa (Tohoku Univ.), Dr. K. Mizuno (IORGC/JAMSTEC), Dr. N. Shikama (IORGC/JAMSTEC), and Prof. T. Suga (Tohoku Univ.) for fruitful comment and discussion on the oceanographic observations. They appreciate great helps of Mr. T. Umeda (JMA) and staff members of JMSDF given when using domestic XBT observations. Thoughtful comments by three anonymous reviewers are thankfully acknowledged. Their appreciation is extended to President H. Iwamiya and Mr. K. Amaike of the Tsurumi Seiki Co. Ltd., for valuable information on a history of XBT. Observational data used in this study are obtained from the following centers: WOA05, WOD05, and GTSPP from NODC/NOAA, tide gauge observation from University of Hawaii Seal Level Center, and JMSDF XBT data from JODC. This work was supported by the Ministry of Education, Culture, Sports, Science and Technology - Japan through the Innovative Program of Climate Change Projection for the 21st Century.

References

AchutaRao, K. M., M. Ishii, B. D. Santer, P. J. Gleckler, K. E. Taylor, T. P. Barnett, D. W. Pierce, R. J. Stouffer, and T. M. L. Wigley (2007): Simulated and observed variability in ocean temperature and heat content. *Proc. Natl. Acad. Sci.*, **104**, 10768 – 10773.

Antonov, J. I., S. Levitus, and T. P. Boyer (2004): Climatological annual cycle of ocean heat content. *Geophys. Res. Lett.*, **31**, L04304, doi:10.1029/2003GL018851.

Boyer, T. P., J. I. Antonov, H. E. Garcia, D. R. Johnson, R. A. Locarnini, A. Mishonov, M. T. Pitcher, O. K. Baranova, and I. V. Smolyar (2006): *World Ocean Database 2005*. NOAA Atlas NESDIS 60, S. Levitus, Ed. (Available at http://www.nodc.noaa.gov/OC5/WOD05/docwod05.html).

Conkright, M. E., R. A. Locarnini, H. E. Garcia, T. D. O. Brien, T. P. Boyer, C. Stephens, and J. I. Antonov (2001): *World Ocean Atlas 2001: Objective Analyses, Data Statistics, and Figures*. NOAA Atlas NESDIS 42. 17 pp., CD-ROM, , U.S. Government Printing Office, Washington, D.C.

Fahrbach, E. (1989): The use of electronic digital thermometers and pressure meters. *WOCE Newsletter No. 8*, pp. 12–13.

Gouretski, V. and K. P. Koltermann (2007): How much is the ocean really warming. *Geophys. Res. Lett.*,, L01610, doi:10.1029/2006GL027834.

Hanawa, K., P. Raul, R. Bailey, A. Sy, and M. Szabados (1995): A new depth-time equation for Sippican or TSK T-7, T-6, and T-4 expendable bathythermographs (XBTs). *Deep Ses Res.*, **42**, 1423–1451.

Ishii, M., M. Kimoto, and M. Kachi (2003): Historical ocean subsurface temperature analysis with error estimates. *Mon. Wea. Rev.*, **131**, 51–73.

Ishii, M., M. Kimoto, K. Sakamoto, and S.-I. Iwasaki (2006): Steric sea level changes estimated from historical subsurface temperature and salinity analyses. *J. Oceanography*, **61**, 155–170.

Kizu, S. and K. Hanawa (2002): Recorder-Dependent Temperature Error of Expendable Bathythermograph. *J. Oceanogr.*, **58**, 469 – 476.

Kizu, S., H. Yoritaka, and K. Hanawa1 (2005): A New Fall-Rate Equation for T-5 Expendable Bathythermograph (XBT) by TSK. *J. Oceanogr.*, **61**, 115 – 121.

Levitus, S. and J. Antonov (1997): *limatological and Interannual Variability of Temperature, Heat Storage, and Rate of Heat Storage in the Upper Ocean*. NOAA Atlas NESDIS 16 186 pp.

Levitus, S., J. I. Antonov, T. P. Boyer, H. E. Garcia, and R. A. Locarnini (2005): Linear trends of zonally averaged thermosteric, halosteric, and total steric sea level for individual ocean basins and the world ocean, (1955–1959)−(1994–1998). *Geophys. Res. Lett.*, **32**, L16601, doi:10.1029/2005GL023761.

Levitus, S., C. Stephens, J. I. Antonov, and T. P. Boyer (2000): *Yearly and year-Season upper ocean temperature anomaly fields, 1948–1998*. NOAA Atlas NESDIS 40. (Available from http://www.nodc.noaa.gov/OC5/PDF/ATLAS/nesdis40.pdf).

Lombard, A., A. Cazenave, P.-Y. Le Traon, and M. Ishii (2005): Contribution of thermal expansion to present-day sea-level change revisited. *Global and Planetary Change*, **47**, 1–16.

Lombard, A., D. Garcia, G. Ramillien, A. Cazenave, R. Biancale, J. M. Lemoine, F. Flechtner, R. Schmidt, and M. Ishii (2007): Estimation of steric sea level variations from combined GRACE and Jason-1 data. *Earth Planet. Sci. Lett.*, **254**, 194–202.

Quadfasel, D., N. Verch, and J. Langhof (1990): Are mercury deep-sea reversing thermometers out of date?. *Ocean Dynamics*,, 145–152.

Reynolds, R. W. and T. M. Smith (1994): Improved global sea surface temperature analyses using optimum interpolation. *J. Climate*, **7**, 929–948.

Sakamoto, T., H. Hasumi, M. Ishii, S. Emori, T. Suzuki, T. Nishimura, and A. Sumi (2005): Responses of the Kuroshio and the Kuroshio Extension to global warming in a high-resolution climate model. *Geophys. Res. Lett.*, **32**, doi:10.1029/2005GL023384.

Smith, D. M. and J. M. Murphy (2007): An objective ocean temperature and salinity analysis using covariances from a global climate model. *J. Geophys. Res.*, **112**, C02022. doi:10.1029/2005JC003172.

Wijffels, S., J. Willis, C. M. Domingues, P. Baker, N. J. White, A. Cronell, K. Ridgway, and J. A. Church (2008): Changing expendable bathythermograph fallrates and their impact on estimates of thermosteric sea level rise. *J. Climate*, (in press).

Willis, J. K., J. M. Lyman, G. C. Johnson, and J. Gilson (2008): In Situ Data Biases and Recent Ocean Heat Content Variability. *J. Atmos. Oceanic Tech.*, (in press).

Willis, J. K., D. Roemmich, and B. Cornuelle (2004): Interannual variability in upper ocean heat content, temperature, and thermosteric expansion on global scales. *J. Geophys. Res.*, **109** C12036, doi:10.1029/2003JC002260.

Wyatt, B., R. Still, D. Barstow, and W. Gilbert (1967): *Hydrographic Data from Oregon Waters 1965*. Depertment Oceanography, School of Science, Oregon State Univ. Date Report No. 27.

Table 1. Fraction of the total number of profiles for each XBT probe type (Frac.; %) stored in the WOD05 and GTSPP data sets for the period from 1966 to 2006, and the number of samples used for constructing equations of the depth-bias correction for each probe type (rightmost column). The total number of profiles is 1,985,888.

No.	XBT type	Frac.[%]	samples
1	T7 (Sippican)	10.6	310,883
2	T4 (Sippican)	22.5	195,679
3	T6 (Sippican)	0.4	18,921
4	T5 (Sippican)	0.4	69,619
5	T10 (Sippican)	1.9	21,824
6	DEEP BLUE (Sippican)	10.0	145,977
7	T4 (TSK)	1.1	8,657
8	T6 (TSK)	0.7	18,099
9	T7 (TSK)	0.8	12,599
10	XBT-7 (Sparton)	0.2	17,194
11	TYPE UNKNOWN	51.3	530,942

Table 2. Coefficient *B* of the time-varying XBT depth bias eqaution (2) defined for individual XBT probe types. Some of probe types are shown by abbreviation; DB and UK denote DEEP BLUE and TYPE UNKNOWN, respectively.

	Sippican						TSK			Sparton	
Year	T7	T4	T6	T5	T10	DB	T4	T6	T7	XBT-7	UK
1966	0.061	0.175	-0.178	0.067	0.059	0.037	0.051	0.014	0.055	-0.317	0.181
1967	0.061	0.175	-0.178	0.067	0.059	0.037	0.051	0.014	0.055	-0.317	0.181
1968	0.061	0.074	-0.178	0.067	0.059	0.037	0.051	0.014	0.055	-0.317	0.184
1969	0.061	0.090	-0.178	0.067	0.059	0.037	0.051	0.014	0.055	-0.317	0.176
1970	0.062	0.102	-0.178	0.067	0.059	0.037	0.051	0.014	0.055	-0.317	0.035
1971	0.143	0.190	-0.178	0.067	0.059	0.037	0.051	0.014	0.055	-0.317	0.093
1972	0.167	0.206	-0.178	0.067	0.059	0.037	0.051	0.014	0.055	-0.317	0.118
1973	0.200	0.228	-0.178	0.067	0.059	0.037	0.051	0.014	0.055	-0.317	0.217
1974	0.177	0.266	-0.178	0.067	0.059	0.037	0.051	0.014	0.055	-0.317	0.184
1975	0.194	0.263	-0.178	0.067	0.059	0.037	0.051	0.014	0.055	-0.317	0.205
1976	0.211	0.305	-0.178	0.067	0.059	0.037	0.051	0.014	0.055	-0.317	0.176
1977	0.234	0.322	-0.178	0.067	0.059	0.037	0.051	0.014	0.055	-0.317	0.333
1978	0.222	0.319	-0.178	0.067	0.059	0.037	0.051	0.014	0.055	-0.317	0.245
1979	0.224	0.319	-0.178	0.067	0.059	0.037	0.051	0.014	0.055	-0.317	0.239
1980	0.217	0.259	-0.178	0.067	0.059	0.037	0.051	0.014	0.055	-0.317	0.197
1981	0.198	0.164	-0.178	0.067	0.059	0.037	0.051	0.014	0.055	-0.317	0.075
1982	0.138	0.124	-0.178	0.067	0.059	0.037	0.051	0.014	0.055	-0.317	0.006
1983	0.136	0.133	-0.178	0.068	0.059	0.037	0.051	0.014	0.055	-0.317	0.046
1984	0.083	0.072	-0.178	0.109	0.059	0.037	0.051	0.014	0.055	-0.317	0.044
1985	0.065	0.081	-0.178	0.109	0.059	0.037	0.051	0.014	0.055	-0.317	0.034
1986	0.036	0.053	-0.178	0.109	0.059	0.037	0.051	0.014	0.055	-0.317	-0.015
1987	0.011	0.063	-0.178	0.109	0.055	0.037	0.051	0.014	0.055	-0.317	-0.019
1988	0.064	0.046	-0.178	0.109	0.056	0.037	0.051	0.014	0.055	-0.317	0.003
1989	0.097	0.022	-0.178	0.109	0.081	0.037	0.051	0.014	0.055	-0.318	0.057
1990	0.105	-0.016	-0.178	0.109	0.082	0.037	0.051	0.014	0.055	-0.318	0.059
1991	0.087	-0.022	-0.178	0.106	0.082	0.037	0.051	0.014	0.055	-0.318	0.060
1992	0.130	-0.040	-0.178	0.127	0.082	0.037	0.051	0.014	0.055	-0.317	0.066
1993	0.128	0.078	-0.178	0.136	0.082	0.031	0.051	0.014	0.055	-0.286	0.074
1994	0.109	0.089	-0.179	0.167	0.089	0.074	0.051	0.014	0.055	-0.258	0.074
1995	0.086	0.101	-0.255	0.095	0.090	0.016	0.051	0.014	0.055	-0.247	0.056
1996	0.061	0.100	-0.244	0.121	0.090	0.032	0.051	0.015	0.055	-0.171	0.033
1997	0.073	0.106	-0.240	0.143	0.100	0.036	0.051	0.015	0.064	-0.171	0.036
1998	0.038	0.121	-0.238	0.170	0.086	0.093	0.051	0.009	0.064	-0.171	0.057
1999	0.057	0.180	-0.239	0.130	0.086	0.128	0.051	-0.004	0.064	-0.171	0.053
2000	0.065	0.183	-0.235	0.142	0.083	0.120	0.051	-0.009	0.065	-0.171	0.123
2001	0.085	0.183	-0.233	0.108	0.055	0.100	0.051	-0.011	0.049	-0.171	0.120
2002	0.098	0.183	-0.233	0.021	0.054	0.095	0.051	0.001	0.039	-0.171	0.120
2003	0.156	0.183	-0.233	0.014	0.054	0.094	0.051	-0.018	0.038	-0.171	0.120
2004	0.172	0.183	-0.233	0.032	0.054	0.086	0.051	-0.017	0.038	-0.171	0.120
2005	0.180	0.183	-0.233	0.032	0.054	0.087	0.051	-0.017	0.038	-0.171	0.120
2006	0.180	0.183	-0.233	0.032	0.054	0.083	0.051	-0.017	0.038	-0.171	0.120

Table 3. Coefficients of the time-varying MBT depth bias equation: $\hat{d} = Dz + Cz^2$. Units of coefficients C and D are $10^{-4}m/m^2$ and $10^{-2}m/m$, respectively. The coefficients before 1950 and after 1994 is the same as those for 1948 and 1996, respexctively.

Year	C	D	Year	C	D
1950	2.71	-0.57			
1951	2.75	-0.66			
1952	2.75	-0.66			
1953	2.76	-0.68			
1954	2.75	-0.66			
1955	2.02	-0.16			
1956	1.98	-0.11	1976	1.64	0.54
1957	1.64	0.04	1977	1.59	0.34
1958	1.61	-0.01	1978	2.96	-0.94
1959	1.87	-0.43	1979	2.30	-0.22
1960	1.64	0.00	1980	2.80	-0.85
1961	1.18	0.51	1981	2.86	-1.02
1962	1.00	0.98	1982	2.61	-1.00
1963	1.05	1.11	1983	2.15	-0.83
1964	1.35	0.90	1984	2.79	-1.44
1965	0.62	1.52	1985	2.22	-1.11
1966	0.59	1.58	1986	1.82	-0.98
1967	0.67	1.36	1987	1.84	-1.17
1968	0.73	1.26	1988	2.02	-1.37
1969	0.33	1.68	1989	2.00	-1.48
1970	1.03	0.80	1990	2.16	-2.07
1971	1.26	0.71	1991	1.72	-1.61
1972	1.14	0.95	1992	1.75	-1.66
1973	1.08	0.88	1993	1.74	-1.65
1974	1.02	0.96	1994	1.56	-1.49
1975	1.27	0.75			

Table 4. Versions of the temperature analysis compared in this study.

Ver.	Changes
6.2	Ishii et al. (2006): use of WOD01 and WOA01, and no XBT and MBT depth bias correction
6.3	Same as ver. 6.2 except use of WOD05 and WOA05
6.6	Same as ver. 6.3 except introduction of XBT and MBT depth bias correction
6.6X	Same as ver. 6.3 except introduction of only XBT depth bias correction
6.7	Same as ver. 6.6 except replacement of temperature climatology

Table 5. Linear trends of global (60˚S–60˚N) annual mean OHC ($10^{22} J/yr$) and thermosteric sea level (mm/yr) estimated from each versions of temperature analysis respectively for a long-term period (1951–2005) and the latest decade (1993–2005).

	OHC		Thermosteric sea level	
Ver.	1951–2005	1993–2005	1951–2005	1993–2005
6.2	0.141 ± 0.035	0.296 ± 0.230	0.300 ± 0.067	0.805 ± 0.448
6.3	0.127 ± 0.035	0.369 ± 0.154	0.262 ± 0.063	0.899 ± 0.304
6.6	0.105 ± 0.034	0.590 ± 0.152	0.236 ± 0.066	1.24 ± 0.298
6.6X	0.075 ± 0.034	0.581 ± 0.152	0.180 ± 0.064	1.23 ± 0.297
6.7	0.147 ± 0.029	0.582 ± 0.151	0.294 ± 0.057	1.23 ± 0.295

Figure captions

Fig. 1

Time series of the number of temperature profiles in which observations are available at depths greater than the 100 *m* depth. The numbers are yearly counts for WOD01 (thin solid) and WOD05 (thick solid). Those for XBT (broken), MBT (dash-dotted), and Argo (dotted) in WOA05 are plotted together.

Fig. 2

Profiles of mean XBT depth biases (thick solid; BIAS), root-mean square differences between XBT and CTD+BOTTLE (dotted; RMSD), and residuals after the correction by using the depth bias equation (thin solid; CORRECTED) for each XBT probe type and MBT. The unit is meter.

Figure size: 100%, please

Fig. 3

Uncertainties expressed by 95% confidence interval in the coefficients of the quadratic equation for the XBT depth biases as a function of the number of pairs of XBT and CTD+BOTTLE. The figure is for the case of unknown XBT probe type, showing its uncertainty averaged over the entire period (1966–2006). Thick solid curve indicates errors in the coefficient of the linear equation. Shading indicates ranges between maximum and minimum 95% confidence levels during the whole period of the statistics. For the case of the quadratic equation, uncertainties in B and A are shown by thin solid and broken curves, respectively. The scale (m/s) for B is shown in the left-hand side and that (m/s^2) for A is in the right-hand side. Horizontal dotted line indicates 95% confidence intervals of Hanawa et al. (1995).

Fig. 4

Time series of coefficient B (m/s) of the linear equation for a) T4 (thick solid) and b) T7 and DEEP BLUE ("D. BLUE" in the figure) of Sippican (thick solid and broken, respectively), compared with those for shallow and deep XBTs given by Wijffels et al. (2008) (thin solid) and with those of *type unknown* (dotted). Values indicated by thin solid curves are obtained after multiplying fractional depth errors (depth error divided by depth) listed in their table by 6.691 which is b of Hanawa et al.'s fall-rate equation. Line of DEEP BLUE before 1992 is not shown since they do not vary over this period.

1 Fig. 5

Uncertainties expressed by 95% confidence interval in the coefficients of the quadratic equation for the MBT depth biases as a function of the number of pairs of MBT and CTD+BOTTLE. Solid and broken curves indicate errors in coefficients D ($10^{-2}m/m$) and C ($10^{-4}m/m^2$), respectively. Thick lines denote the averages over a period from 1945–2003, and the lower and upper lines respectively show minimum and maximum in the period of statistics. Horizontal dotted line is equivalent to that in Fig. 3, that is 95% confidence intervals of Hanawa et al. (1995).

2 Fig. 6

Geographical distribution of difference in ocean heat content (OHC) computed from temperature analyses of ver. *6.6* minus ver. *6.3*. The negative differences are shaded. The difference at each grid is normalized by the standard deviation of the interannual variation of OHC. Circles indicate the locations of the tide gauge stations used for the verification in Fig. 8.

3 Fig. 7

Time series of annual global mean ocean heat contents ($10^{22}J$) computed from the previous (ver. *6.2*; V6.2; thin solid) and present temperature analyses: dotted for ver. *6.3* (V6.3), dash-dotted for ver. *6.6* (V6.6), and thick solid for ver. *6.7* (V6.7), integrated from sea surface to 700 *m* depth. Shading denotes one-sigma errors, following the curve of the ver. *6.7* OHC. Changes in OHC by the MBT depth bias correction are denoted by line with solid circles in the lower part of the figure. The values are differences ($10^{22}J$) between the ver. *6.6* and *6.6X* analyses, and the scale is shown in the right hand side of the figure. A binomial filter with weights 0.25, 0.5, and 0.25, is applied to all time series in the figure for a better visibility of their differences. The ver. *6.2* (V6.2) OHC is padded by $11 \times 10^{22}J$ that is originated from the difference of climatology, WOA01 and WOA05, used in the objective analysis. Figure size: 100%, please

Fig. 8

Time series of monthly tide gauge sea level anomaly (dotted) and thermosteric sea level anomalies estimated from the ver. *6.3* analysis without the XBT and MBT depth bias correction (thin solid) and from that of the ver. *6.7* with the correction. The values are 13-month running means of sea level at tide gauge stations available in latitudes from 30˚S to 30˚N of the Pacific Ocean (marked by circles in Fig. 6). Bars denote the number of tide gauge stations available for each month, and its scale is shown on the right-hand side.

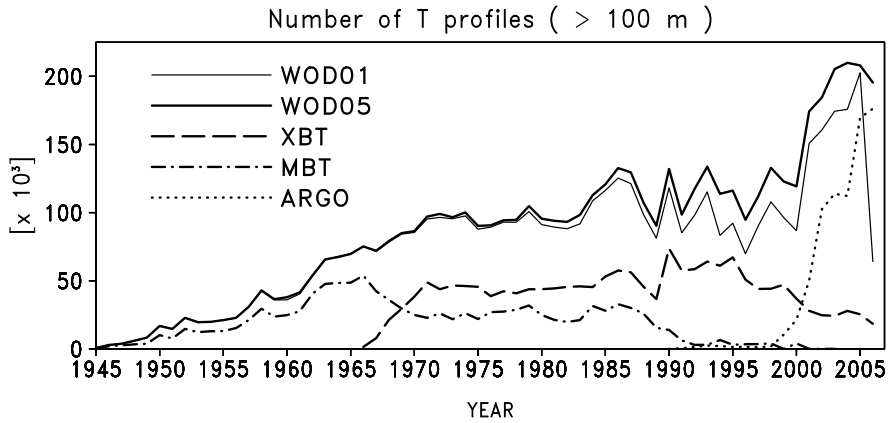

Fig. 1. Time series of the number of temperature profiles in which observations are available at depths greater than the 100 *m* depth. The numbers are yearly counts for WOD01 (thin solid) and WOD05 (thick solid). Those for XBT (broken), MBT (dash-dotted), and Argo (dotted) in WOA05 are plotted together.

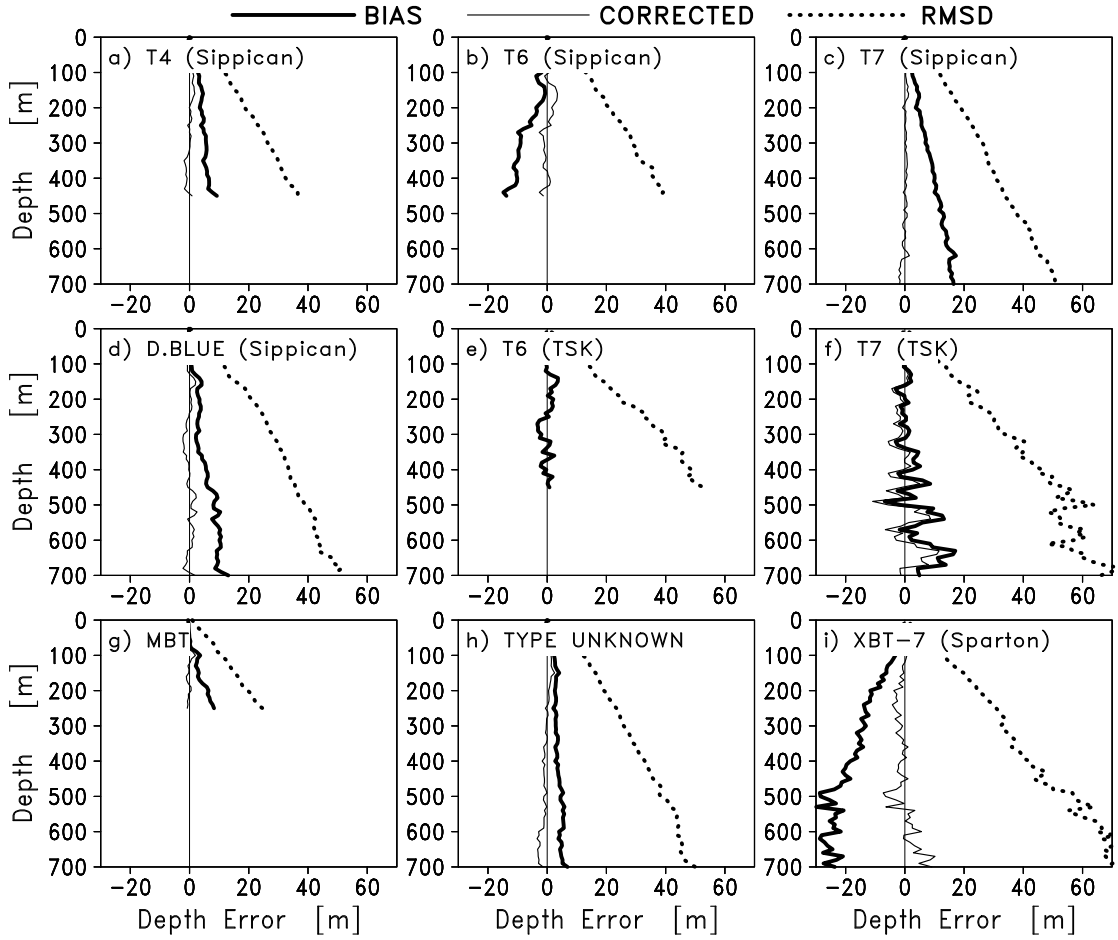

Fig. 2. Profiles of mean XBT depth biases (thick solid; BIAS), root-mean square differences between XBT and CTD+BOTTLE (dotted; RMSD), and residuals after the correction by using the depth bias equation (thin solid; CORRECTED) for each XBT probe type and MBT. The unit is meter. Figure size 100%, please.

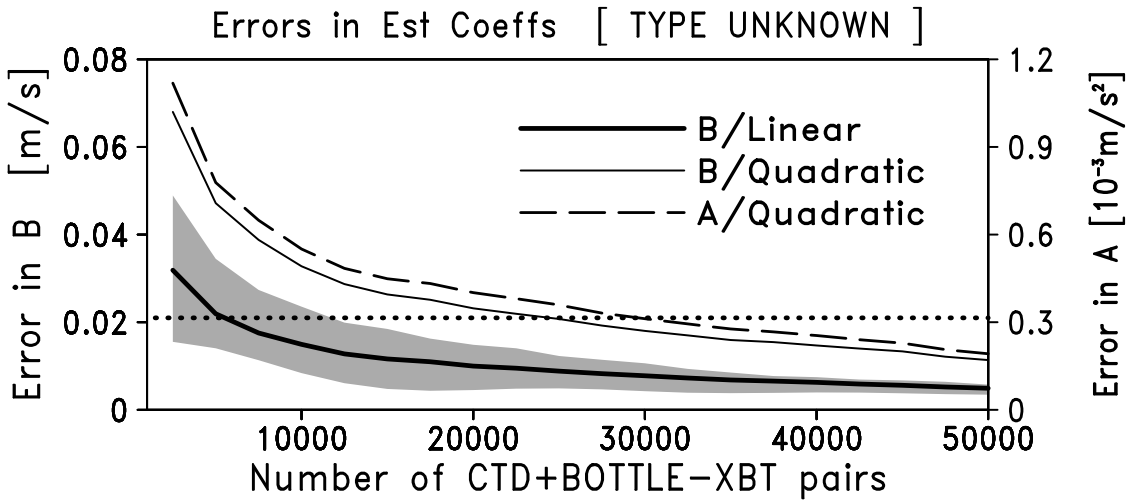

Fig. 3. Uncertainties expressed by 95% confidence interval in the coefficients of the quadratic equation for the XBT depth biases as a function of the number of pairs of XBT and CTD+BOTTLE. The figure is for the case of unknown XBT probe type, showing its uncertainty averaged over the entire period (1966–2006). Thick solid curve indicates errors in the coefficient of the linear equation. Shading indicates ranges between maximum and minimum 95% confidence levels during the whole period of the statistics. For the case of the quadratic equation, uncertainties in B and A are shown by thin solid and broken curves, respectively. The scale (m/s) for B is shown in the left-hand side and that (m/s^2) for A is in the right-hand side. Horizontal dotted line indicates 95% confidence intervals of Hanawa et al. (1995).

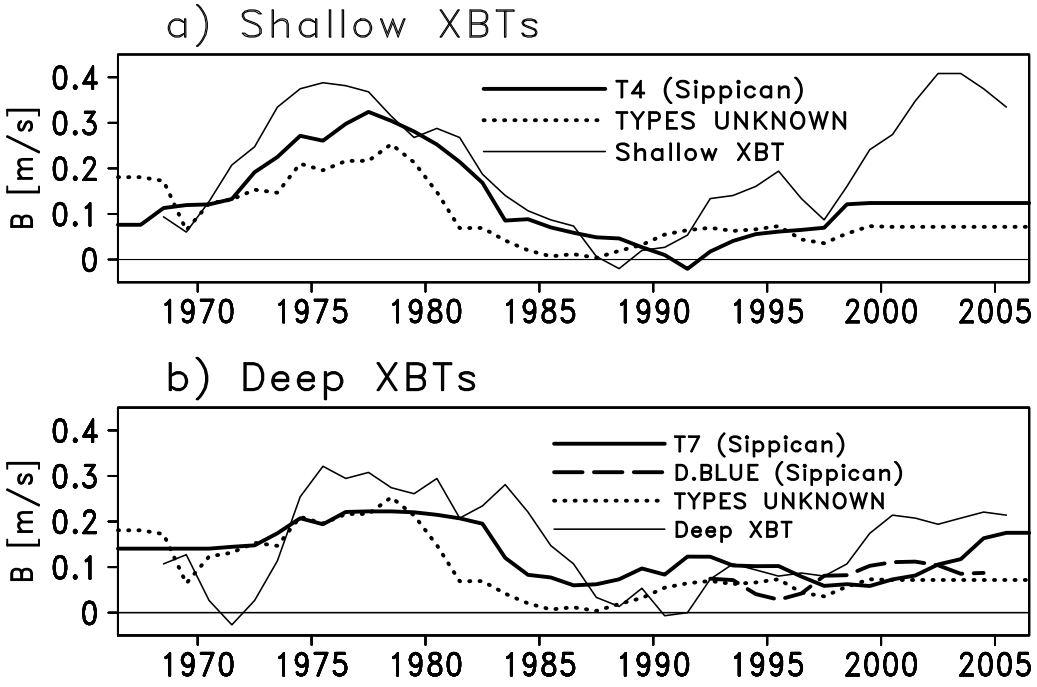

Fig. 4. Time series of coefficient B (m/s) of the linear equation for a) T4 (thick solid) and b) T7 and DEEP BLUE ("D. BLUE" in the figure) of Sippican (thick solid and broken, respectively), compared with those for shallow and deep XBTs given by Wijffels et al. (2008) (thin solid) and with those of *type unknown* (dotted). Values indicated by thin solid curves are obtained after multiplying fractional depth errors (depth error divided by depth) listed in their table by 6.691 which is b of Hanawa et al.'s fall-rate equation. Line of DEEP BLUE before 1992 is not shown since they do not vary over this period.

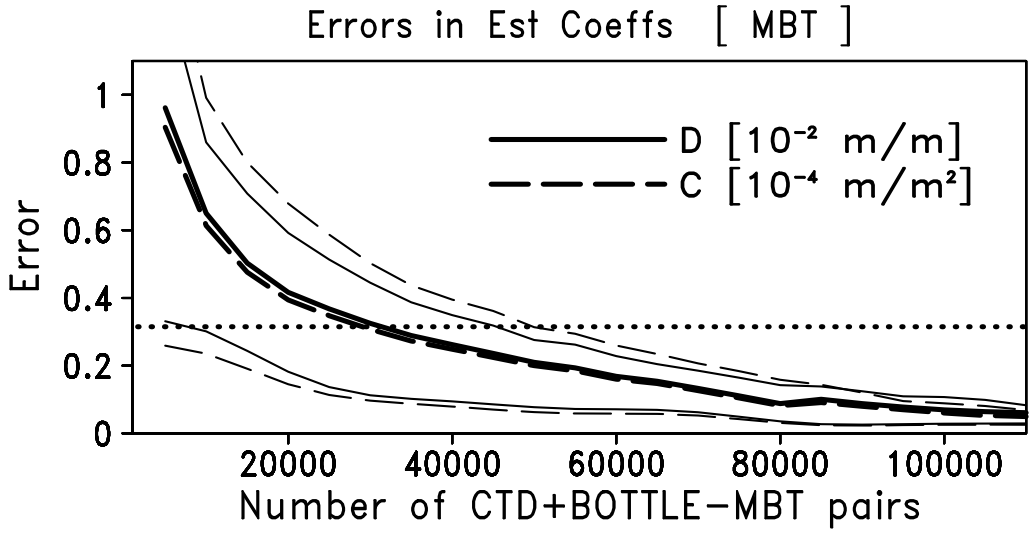

Fig. 5. Uncertainties expressed by 95% confidence interval in the coefficients of the quadratic equation for the MBT depth biases as a function of the number of pairs of MBT and CTD+BOTTLE. Solid and broken curves indicate errors in coefficients D ($10^{-2}m/m$) and C ($10^{-4}m/m^2$), respectively. Thick lines denote the averages over a period from 1945–2003, and the lower and upper lines respectively show minimum and maximum in the period of statistics. Horizontal dotted line is equivalent to that in Fig. 3, that is 95% confidence intervals of Hanawa et al. (1995).

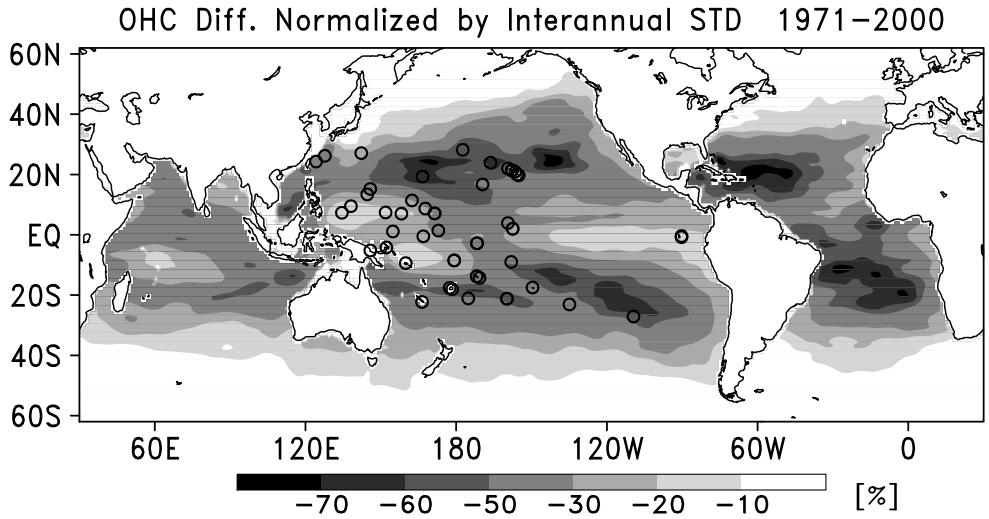

Fig. 6. Geographical distribution of difference in ocean heat content (OHC) computed from temperature analyses of ver. *6.6* minus ver. *6.3*. The negative differences are shaded. The difference at each grid is normalized by the standard deviation of the interannual variation of OHC. Circles indicate the locations of the tide gauge stations used for the verification in Fig. 8.

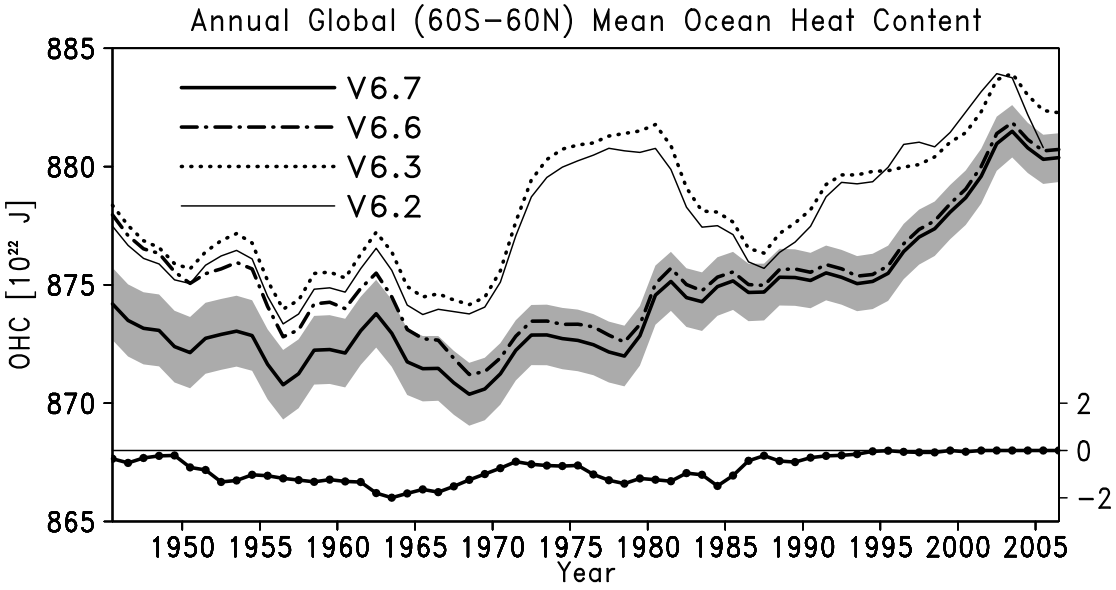

Fig. 7. Time series of annual global mean ocean heat contents ($10^{22}J$) computed from the previous (ver. *6.2*; V6.2; thin solid) and present temperature analyses: dotted for ver. *6.3* (V6.3), dash-dotted for ver. *6.6* (V6.6), and thick solid for ver. *6.7* (V6.7), integrated from sea surface to 700 *m* depth. Shading denotes one-sigma errors, following the curve of the ver. *6.7* OHC. Changes in OHC by the MBT depth bias correction are denoted by line with solid circles in the lower part of the figure. The values are differences ($10^{22}J$) between the ver. *6.6* and *6.6X* analyses, and the scale is shown in the right hand side of the figure. A binomial filter with weights 0.25, 0.5, and 0.25, is applied to all time series in the figure for a better visibility of their differences. The ver. *6.2* (V6.2) OHC is padded by $11 \times 10^{22}J$ that is originated from the difference of climatology, WOA01 and WOA05, used in the objective analysis. Figure size 100%, please.

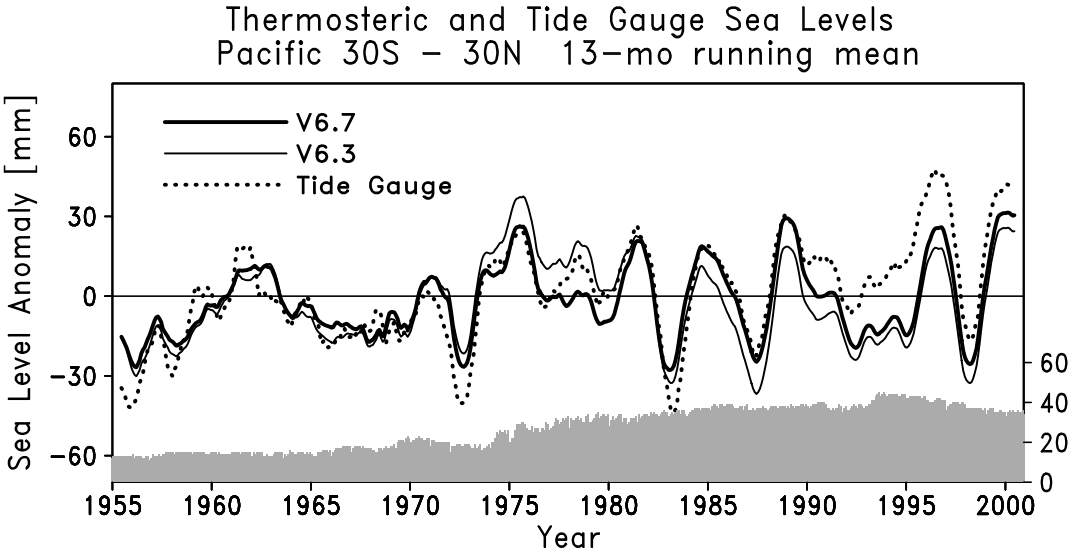

Fig. 8. Time series of monthly tide gauge sea level anomaly (dotted) and thermosteric sea level anomalies estimated from the ver. *6.3* analysis without the XBT and MBT depth bias correction (thin solid) and from that of the ver. *6.7* with the correction. The values are 13-month running means of sea level at tide gauge stations available in latitudes from 30˚S to 30˚N of the Pacific Ocean (marked by circles in Fig. 6). Bars denote the number of tide gauge stations available for each month, and its scale is shown on the right-hand side.